

# GENERALIZED FILTERED BACKPROJECTION IN NONLINEAR ACOUSTICS

*D. Russell Luke*

University of Delaware  
Department of Mathematical Sciences  
Newark DE 19716-2553, USA

## ABSTRACT

The filtered backprojection algorithm (FBP) is a standard image reconstruction algorithm used in many imaging modalities. The FBP algorithm is suited for high-frequency imaging applications, that is, applications where the specimen is much larger than the wavelengths of the incident fields. However, when data is scarce due to limited view or dosage considerations, or when super-resolution is required, different techniques are needed to adequately resolve the specimen. We present a generalization of the filtered backprojection algorithm that extends the capabilities of acoustic imaging systems to limited aperture and wavelength resolution. Our principal interest is applications to acoustic (scalar) scattering, though the methodology we develop can be extended to general electromagnetic (vector) settings.

## 1. INTRODUCTION

Many innovative algorithms have appeared in recent years for inverse scattering applications with single-, low-frequency applications in mind. Good examples can be found in the work of Colton and Kirsch [1], Potthast [2] and Colton and Kress [3]. In the present work, we extend the Point Source Method of Potthast [2] to a multifrequency framework in order to derive a generalization of the well known filtered backprojection (FBP) algorithm for acoustic imaging. The difference between the generalization and conventional FBP is the region of validity: conventional FBP works best at high frequencies, while the generalized FBP (GFBP) is not limited by frequency. This opens the door to super-resolution capabilities for systems that currently rely on conventional FBP-based image reconstruction.

## 2. SCATTERING MODEL

As a matter of convenience, our discussion is limited to scattering of small-amplitude, time-harmonic waves from an

---

This work was supported in part by the University of Göttingen and in part by the Pacific Institute for the Mathematical Sciences at Simon Fraser University.

impenetrable, sound-soft obstacle embedded in an isotropic homogeneous medium. The techniques described here are easily adapted to obstacles with Neumann and impedance boundaries and to electromagnetic scattering. Extensions to inhomogeneous media are a topic of current research.

The obstacle is identified by its support  $\Omega \subset \mathbb{R}^m$ ,  $m = 2$  or  $3$  and is a bounded domain with connected, piecewise smooth  $\partial\Omega$  and the unit outward normal  $\nu$ . We illuminate this obstacle with an *incident field*, denoted by  $v^i : \mathbb{R}^m \rightarrow \mathbb{C}$ , that satisfies Eq.(1) on  $\mathbb{R}^m$ . The *total field*, denoted by  $v$ , is the superposition of the *scattered field*  $v^s$  and the incident field  $v^i$ . The governing equation for this setting is the Helmholtz equation with sound-soft (Dirichlet) boundary conditions and the Sommerfeld radiation condition

$$(\Delta + \kappa^2) v(x) = 0, \quad x \in \overline{\Omega}^c \subset \mathbb{R}^m, \quad (1)$$

$$v = 0 \quad \text{on } \partial\Omega, \quad (2)$$

$$v = v^i + v^s, \quad (3)$$

$$r^{\frac{m-1}{2}} \left( \frac{\partial}{\partial r} - i\kappa \right) v^s(x) \rightarrow 0, \quad r = |x| \rightarrow \infty, \quad (4)$$

where  $\Delta$  denotes the Laplacian,  $\kappa \geq 0$  is the *frequency* or *wavenumber* and  $\overline{\Omega}^c := \mathbb{R}^m \setminus \overline{\Omega}$ .

At large distances from the obstacle  $\Omega$ , the scattered field  $v^s$  is characterized by the *far field pattern*  $v^\infty : \mathbb{S} \rightarrow \mathbb{C}$  on the set of directions  $\mathbb{S} := \{x \in \mathbb{R}^m \mid |x| = 1\}$ . We denote the direction of a vector  $x \in \mathbb{R}^m$  by  $\hat{x} := x/|x|$ .

Denote the free-space fundamental solution to Eq.(1) by  $\Phi : \mathbb{R}^m \times \mathbb{R}^m \rightarrow \mathbb{C}$  (see [Eq.(3.60) and Eq.(2.1)] [3]). Then  $v^s$  satisfies Green's formula [3, Eq.2.5], also known as the Integral Theorem of Kirchhoff and Helmholtz, for  $x \in \overline{\Omega}^c$  and  $\kappa > 0$ . Green's formula applied to  $v^s$ , together with Green's Theorem applied to  $v^i$  and  $\Phi$ , yield the following formalization of Huygens's principle [3, Thm. 3.12]

$$v^s(x) = - \int_{\partial\Omega} \frac{\partial v(z)}{\partial \nu(z)} \Phi(x, z) ds(z), \quad x \in \overline{\Omega}^c. \quad (5)$$

The corresponding far-field pattern is given by

$$v^\infty(\hat{x}) = -\beta \int_{\partial\Omega} \frac{\partial v(z)}{\partial \nu(z)} e^{-i\kappa \hat{x} \cdot z} ds(z), \quad \hat{x} \in \mathbb{S}. \quad (6)$$

where  $\beta$  is given by [3, Eq.(2.13) and Eq.(3.64)]

$$\beta = \frac{e^{-i\frac{\pi}{4}}}{\sqrt{8\pi\kappa}}, \quad \text{for } m = 2 \quad \text{and} \quad \beta = \frac{1}{4\pi}, \quad \text{for } m = 3. \quad (7)$$

Note that in two dimensions,  $\beta$  is a function of  $\kappa$ , unlike the three dimensional setting. We reserve special notation for incident *plane waves* denoted by

$$u^i(x, \hat{\eta}) := e^{i\kappa x \cdot \hat{\eta}}, \quad x \in \mathbb{R}^m, \quad \hat{\eta} \in \mathbb{S}. \quad (8)$$

Here  $\hat{\eta} \in \mathbb{S}$ , indicates the *direction of incidence*.

### 3. INVERSE SCATTERING

In inverse scattering, we wish to reconstruct the boundary of the scatterer,  $\partial\Omega$ , from measurements of the far field on an array of receptors located on  $\Gamma$ , a subset of all possible view angles on  $\mathbb{S}$ . The central idea is to project the far field measurements back to the surface of the scatterer, hence the name *backprojection*. There are two key ingredients to accomplish this. The first is the familiar Green's formula. The second ingredient is the superposition of plane waves known as the Herglotz wave function.

By Green's formula we have

$$v^s(x) = \int_{\partial\Omega} \left\{ \Phi(x, y) \frac{\partial v^s}{\partial \nu}(y) - \frac{\partial \Phi(x, y)}{\partial \nu(y)} v^s(y) \right\} ds(y), \quad (9)$$

for  $x \in \bar{\Omega}^c$ . In the far field, that is, as  $|x| \rightarrow \infty$ , this becomes

$$v^s(\hat{x}) = \beta \int_{\partial\Omega} \left\{ e^{-i\kappa \hat{x} \cdot y} \frac{\partial v^s}{\partial \nu}(y) - \frac{\partial e^{-i\kappa \hat{x} \cdot y}}{\partial \nu(y)} v^s(y) \right\} ds(y). \quad (10)$$

The *Herglotz wave function with density  $g$*  is defined by

$$h_g(x) = \int_{\Gamma} e^{i\kappa x \cdot (-\hat{y})} g(-\hat{y}) ds(\hat{y}) \quad (11)$$

for  $x \in \mathbb{R}^m$ ,  $\Gamma \subset \mathbb{S}$ . Since the related Herglotz wave operator is injective with dense range [2], by appropriately choosing the density  $g$ , we can construct a function of the form Eq.(11) that approximates any square integrable function arbitrarily closely on curves. The idea for constructing a backprojector, then, is to use  $h_g(x)$  to approximate  $\Phi(x, z)$  on  $\partial\Omega$ . By Green's Formula and Eq.(9)-(11), for  $z \in \mathbb{R}^m \setminus \bar{\Omega}$ ,

$$\begin{aligned} v^s(z) &= \int_{\partial\Omega} \left\{ \Phi(x, z) \frac{\partial v^s}{\partial \nu}(x) - \frac{\partial \Phi(x, z)}{\partial \nu(x)} v^s(x) \right\} ds(x), \\ &\approx \int_{\partial\Omega} \left\{ h_g(x) \frac{\partial v^s}{\partial \nu}(x) - \frac{\partial h_g(x)}{\partial \nu(x)} v^s(x) \right\} ds(x), \\ &= \int_{\Gamma} v^\infty(\hat{\eta}) \frac{g(-\hat{\eta})}{\beta} ds(\hat{\eta}). \end{aligned} \quad (12)$$

We thus define the *backprojector*

$$(\mathcal{A}_g v^\infty)(z, \kappa) := \int_{\Gamma} v^\infty(\hat{y}, \kappa) \frac{g(-\hat{y}, z, \kappa)}{\beta(\kappa)} ds(\hat{y}). \quad (13)$$

Here we have allowed for the possibility of polychromatic scattering by explicitly including the dependence on the frequency  $\kappa$ . Then

$$(\mathcal{A}_g v^\infty)(z, \kappa) \approx v^s(z, \kappa)$$

where, for fixed  $z \in \bar{\Omega}^c$  and  $\kappa$ , the density  $g$  satisfies

$$\int_{\Gamma} e^{i\kappa x \cdot (-\hat{y})} g(-\hat{y}, z, \kappa) ds(\hat{y}) \approx \Phi(x, z, \kappa)$$

at points on the unknown boundary of the obstacle,  $x \in \partial\Omega$ .

The advantages and challenges of this idea are immediately clear. On one hand, the backprojector maps the far field measurements  $v^\infty$  to *any* point  $z$  on the exterior of the scatterer, for all frequencies, regardless of the boundary condition. We can then use this information to find  $\Omega$ . On the other hand, the best density  $g$  is one that gives the best approximation to  $\Phi(\cdot, z)$  on  $\partial\Omega$ , the unknown boundary.

#### 3.1. The Point Source Method

To circumvent the problem of approximating the fundamental solution on the unknown boundary of the scatterer, we construct density  $g$  by translations and rotations of an *approximating domain*  $\Omega_0$ . The point source method of Potthast [2] is based on the following observation.

**THEOREM 3.1 (POTTHAST, 1996)** *Let  $\Omega_0 \subset \mathbb{R}^m$  be a bounded domain (the domain of approximation) with connected  $C^2$  boundary such that  $\bar{\Omega} \subset \Omega_0$ . Consider scattering from an incident plane wave  $u^i(\cdot, \hat{\eta}, \kappa)$  with direction of incidence  $\hat{\eta}$  and (almost any) frequency  $\kappa > 0$ . Let  $u^s(z, \hat{\eta}, \kappa)$  denote the corresponding scattered field at an arbitrary point  $z \in \bar{\Omega}^c$ , and let  $\Phi(\cdot, z, \kappa)$  denote the fundamental solution at frequency  $\kappa$  due to a point source at  $z$ . The backprojector  $\mathcal{A}_g$  reconstructs  $u^s(z, \hat{\eta}, \kappa)$  arbitrarily closely using any density  $g$  for which the Herglotz wave function  $h_g(\cdot, z, \kappa)$  defined by Eq.(11) approximates  $\Phi(\cdot, z, \kappa)$  sufficiently accurately on  $\Omega_0$ .*

We briefly sketch a method for constructing the density  $g$ . In this short space it is not possible to fully detail the numerical realization of the point source method. Interested readers are referred to [4] and references therein.

**PROPOSITION 3.2** *Let  $\Omega_0 \subset \mathbb{R}^m \setminus \{0\}$  with connected  $C^2$  boundary. Consider*

$$\begin{aligned} \min \quad & \left\| \Phi(\cdot, 0, \kappa) - h_g(\cdot, 0, \kappa) \right\|_{L^2(\partial\Omega_0)}^2 + \alpha_0 \left\| g(\cdot, 0, \kappa) \right\|_{L^2(\mathbb{S})}^2 \\ & + \tilde{\alpha}_0 \left\| (1 - \mathcal{X}_{-\Gamma}) g(\cdot, 0, \kappa) \right\|_{L^2(\mathbb{S})}^2 \end{aligned} \quad (14)$$

over  $g(\cdot, 0, \kappa) \in L^2(\mathbb{S})$ . This problem has a unique solution  $g_*(\cdot, 0, \kappa)$ .

Moreover, the optimal solution to the problem

$$\min \left\| \Phi(\cdot, z, \kappa) - h_g(\cdot, z, \kappa) \right\|_{L^2(\partial(\Omega_0+z))}^2 + \alpha_0 \left\| g(\cdot, z, \kappa) \right\|_{L^2(\mathbb{S})}^2 + \tilde{\alpha}_0 \left\| (1 - \mathcal{X}_{-\Gamma})g(\cdot, z, \kappa) \right\|_{L^2(\mathbb{S})}^2 \quad (15)$$

over  $g(\cdot, z, \kappa) \in L^2(\mathbb{S})$  is given by

$$g_*(\hat{x}, z, \kappa) = e^{-i\kappa z \cdot \hat{x}} g_*(\hat{x}, 0, \kappa), \quad \hat{x} \in \mathbb{S}. \quad (16)$$

According to this theorem, one strategy for constructing a density  $g_*$  is to solve the optimization problem Eq.(14) at each frequency for the optimal density at the origin  $g_*(\cdot, 0, \kappa)$ . The solution to this problem can be written in closed form as the solution to the normal equations. The optimal density at arbitrary points  $z$  is then obtained by Eq.(16), which is just a phase shift of  $g_*(\cdot, 0, \kappa)$ .

Using this density, the backprojection operator given by Eq.(13) corresponding to these translated domains can be written in terms of the generating density  $g_*(\cdot, 0)$  as

$$(\tilde{\mathcal{A}}_{g_*} u^\infty)(z, \hat{\eta}, \kappa) := \int_{\Gamma} u^\infty(\hat{y}, \hat{\eta}, \kappa) \frac{g_*(-\hat{y}, 0, \kappa)}{\beta} e^{-i\kappa z \cdot (-\hat{y})} ds(\hat{y}), \quad (17)$$

for  $z \in \mathbb{R}^m$ . The points  $z$  satisfying the hypotheses of Theorem 3.1 depend on the geometry of the approximating domain  $\Omega_0$  and that of the scatterer  $\Omega$ .

#### 4. PHYSICAL OPTICS AND FILTERED BACKPROJECTION

In this section, we derive conventional filtered backprojection as an approximation of the multifrequency extension of Eq.(17). In [5] it was shown that the solution  $\varphi$  to the integral equation

$$\frac{1}{2(2\pi)^{m/2}} \int_{\Omega^c} u(z, \hat{\eta}, \kappa) e^{i\kappa \hat{\eta} \cdot z} \varphi(z) dz = -\frac{u^\infty(-\hat{y}, \hat{\eta}, \kappa)}{\beta \kappa^2} \quad (18)$$

is given by

$$\varphi(z) = -\frac{1}{2(2\pi)^{m/2}} \Delta \times \left( \int_{\mathbb{R}} \kappa^{m-3} \int_{\mathbb{S}} \bar{u}(z, \hat{\eta}, \kappa) e^{-i\kappa \hat{\eta} \cdot z} \frac{u^\infty(-\hat{y}, \hat{\eta}, \kappa)}{\beta \kappa^2} ds(\hat{\eta}) d\kappa \right) \quad (19)$$

where  $u(z, \hat{\eta}, \kappa) = u^i(z, \hat{\eta}, \kappa) + u^s(z, \hat{\eta}, \kappa)$ . It is apparent from Eq.(18) and Eq.(19) that  $\varphi$  and  $u^\infty$  are a transform pair.

To gain some insight into the nature of this transform, recall the commonly employed physical optics approximation (also known as the weak scattering or Born approximation in inhomogeneous media scattering),

$$u(z, \hat{\eta}, \kappa) \approx u^i(z, \hat{\eta}, \kappa) \quad \text{where} \quad u^i(z, \hat{\eta}, \kappa) = e^{i\kappa z \cdot \hat{\eta}}.$$

Using this approximation in Eq.(18) and Eq.(19) yields

$$\varphi(z) \approx -\frac{1}{2(2\pi)^{m/2}} \times \int_{\mathbb{R}} \int_{\mathbb{S}} \frac{u^\infty(-\hat{y}, \hat{\eta}, \kappa)}{\beta \kappa^2} e^{-i\kappa(\hat{y}+\hat{\eta}) \cdot z} ds(\hat{\eta}) |\kappa|^{m-1} d\kappa \quad (20)$$

and

$$\frac{1}{2(2\pi)^{m/2}} \int_{\Omega^c} e^{i\kappa z \cdot (\hat{y}+\hat{\eta})} \varphi(z) dz \approx -\frac{u^\infty(-\hat{y}, \hat{\eta}, \kappa)}{\beta \kappa^2}. \quad (21)$$

Note that Eq.(20) is a Fourier transform in polar coordinates. Thus,  $-\frac{u^\infty(-\hat{y}, \hat{\eta}, \kappa)}{\beta \kappa^2}$  and  $\varphi$  are a (weighted) Fourier transform pair on the physical domain  $\bar{\Omega}^c$ .

The variable  $\hat{y}$  in Eq.(20) is arbitrary, thus we can change variables on the inner integral to obtain an equivalent integral

$$\int_{\mathbb{S}} \frac{u^\infty(-\hat{\eta}, \hat{x}, \kappa)}{\beta \kappa^2} e^{-i\kappa(\hat{x}+\hat{\eta}) \cdot z} ds(\hat{x}).$$

By a standard reciprocity relation,

$$u^\infty(-\hat{\eta}, \hat{x}, \kappa) = u^\infty(-\hat{x}, \hat{\eta}, \kappa). \quad (22)$$

This, together with another change of variables ( $\hat{x} = -\hat{y}$ ) yields the filtered backprojection operator that is recurrent in computed tomography applications:

$$\varphi(z) \approx \frac{1}{2(2\pi)^{m/2}} \times \int_{\mathbb{R}} \int_{\mathbb{S}} u^\infty(\hat{y}, \hat{\eta}, \kappa) \frac{e^{-i\kappa(\hat{\eta}-\hat{y}) \cdot z}}{\beta \kappa^2} ds(\hat{y}) |\kappa|^{m-1} d\kappa. \quad (23)$$

Comparing the inner integral of Eq.(23) with Eq.(13), it is apparent that Eq.(23) is a superposition of backprojection operators  $\mathcal{A}_g$  over all frequencies. Indeed, we can write the above expression more compactly as

$$\varphi(z) \approx \int_{\mathbb{R}} (\tilde{\mathcal{A}}_{\bar{g}} u^\infty)(z, \hat{\eta}, \kappa) |\kappa|^{m-1} d\kappa \quad (24)$$

where

$$\begin{aligned} (\tilde{\mathcal{A}}_{\bar{g}} u^\infty)(z, \hat{\eta}, \kappa) &:= \int_{\mathbb{S}} u^\infty(\hat{y}, \hat{\eta}, \kappa) \frac{e^{-i\kappa z \cdot (\hat{\eta}-\hat{y})}}{2(2\pi)^{m/2} \beta \kappa^2} ds(\hat{y}) \\ &\approx u^s(z, \hat{\eta}, \kappa) \end{aligned} \quad (25)$$

for the density, or *filter*

$$\tilde{g}(\hat{y}, z, \kappa, \hat{\eta}) = \frac{\beta e^{-i\kappa z \cdot (\hat{\eta}+\hat{y})}}{2(2\pi)^{m/2} \beta \kappa^2}. \quad (26)$$

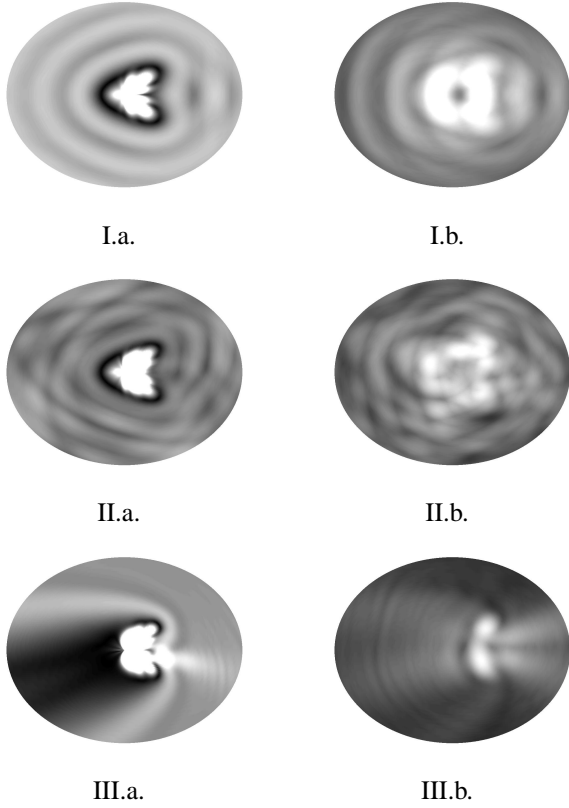


**Fig. 1.** Full aperture, ( $\Gamma = \mathbb{S}$  sampled at 128 points) reconstructions for three different regimes: I.a.-b. 1 incident field, and 16 wavenumbers evenly spaced on the interval  $[0, 6]$ ; II.a.-b. 4 incident fields evenly spaced on the interval  $[0, 2\pi]$ , and 4 wavenumbers evenly spaced on the interval  $[0, 6]$ ; III.a.-b. 16 incident fields evenly spaced on the interval  $[0, 2\pi]$ , and 1 wavenumber,  $\kappa = 2$ . The optimized density Eq.(16) was used in reconstruction (a) and the physical optics approximation density Eq.(26) was used in reconstruction (b)

This filter is dependent on the incident direction  $\hat{\eta}$ . Note that the aperture  $\Gamma$  in this derivation is the entire sphere  $\mathbb{S}$ . This is an artifact of the use of the eigenfunction expansion theorem that was used to derive Eq.(19) (see [5]), but the theory is not limited to this setting.

## 5. NUMERICAL RESULTS

Reconstructions using generalized filtered backprojection are accomplished in the following series of steps.

ALGORITHM 5.1 (GENERALIZED FBP) :

**Step 1:** (Generating density  $g_*(\hat{y}, 0, \kappa)$ ): Set up the generating approximation domain  $\Omega_0$  and, at each frequency  $\kappa_k$ , solve the minimization problem Eq.(14) or

Eq.(15) for the generating density  $g_*(-\hat{y}_l, 0, \kappa_k)$  corresponding to the far field measurements  $u^\infty(\hat{y}_l, \hat{\eta}, \kappa_k)$  ( $l, k \in \mathbb{N}$ ).

**Step 2:** (Backprojection) At points  $z_i \in \mathcal{G}$  ( $i \in \mathbb{N}$ ), the computational grid, calculate the approximation to the scattered field  $u_*^s(z_i, \hat{\eta}_j, \kappa_k)$  for each direction  $\hat{\eta}_j$ , ( $j \in \mathbb{N}$ ) and each frequency  $\kappa_k$ , ( $k \in \mathbb{N}$ ).

**Step 3:** (Integration) Add the modulus squared of all approximated total fields, that is, for each  $z_i$  compute  $f(z_i)$  defined by

$$f(z_i) = \sum_{k=1}^K \sum_{j=1}^J \left| u_*^s(z_i, \hat{\eta}_j, \kappa_k) + u^i(z_i, \hat{\eta}_j, \kappa_k) \right|^2. \quad (27)$$

For our simulations we use a kite-shaped sound-soft obstacle used in [3, Section 3.5] and incident waves with wavelength on the order of magnitude of the obstacle. Reconstructions with the point source method are shown with densities  $g_*$  calculated via the optimization problem Eq.(16). In each, the regularization parameter  $\alpha = 10^{-8}$  and the penalty parameter  $\tilde{\alpha} = \infty$ . These reconstructions are compared to reconstructions using the physical optics density  $\tilde{g}$  (see Eq.(26)) in Step 2. of Algorithm 5.1, rather than  $g_*$ . In each of the experiments, the same number of data points is used, that is, the number of far field measurements times the number of incident fields times the number of frequencies used is always equal to 2048.

## 6. REFERENCES

- [1] D. Colton and A. Kirsch, "A simple method for solving inverse scattering problems in the resonance region," *Inverse Problems*, vol. 12, no. 4, pp. 383–93, 1996.
- [2] R. Potthast, "A fast new method to solve inverse scattering problems," *Inverse Problems*, vol. 12, pp. 731–42, 1996.
- [3] D. Colton and R. Kress, *Inverse Acoustic and Electromagnetic Scattering Theory*, Springer-Verlag, New York, 2nd edition, 1998.
- [4] D. R. Luke, "Multifrequency inverse obstacle scattering: the point source method and generalized filtered backprojeciton," *Math. and Computers in Simulation*, vol. 66, no. 4–5, pp. 297–314, 2004.
- [5] D. R. Luke, "Image synthesis for inverse obstacle scattering using the eigenfunction expansion theorem," *J. on Computing*, to appear.